Received: 8 May 2022 | Revised: 11 July 2022 | Accepted: 22 August 2022

DOI: 10.1002/hbm.26073

RESEARCH ARTICLE

WILEY

Early effect of thrombolysis on structural brain network organisation after anterior-circulation stroke in the randomized WAKE-UP trial

Eckhard Schlemm[1] | Märit Jensen[1] | Amy Kuceyeski[2] | Keith Jamison[2] | Thies Ingwersen[1] | Carola Mayer[1] | Alina Königsberg[1] | Florent Boutitie[2,3,4,5] | Martin Ebinger[6,7] | Matthias Endres[6,8,9,10,11] | Jochen B. Fiebach[6] | Jens Fiehler[12] | Ivana Galinovic[6] | Robin Lemmens[13,14,15] | Keith W. Muir[16] | Norbert Nighoghossian[17] | Salvador Pedraza[18] | Josep Puig[18] | Claus Z. Simonsen[19] | Vincent Thijs[20,21] | Anke Wouters[13,14,15,22] | Christian Gerloff[1] | Götz Thomalla[1] | Bastian Cheng[1]

[1]Klinik und Poliklinik für Neurologie, Kopf- und Neurozentrum, University Medical Centre Hamburg-Eppendorf, Hamburg, Germany

[2]Department of Radiology, Weill Cornell Medicine, New York, New York, USA

[3]Hospices Civils de Lyon, Service de Biostatistique, Lyon, France

[4]Université Lyon 1, Villeurbanne, France

[5]CNRS, UMR 5558, Laboratoire de Biométrie et Biologie Evolutive, Equipe Biostatistique-Santé, Villeurbanne, France

[6]Centrum für Schlaganfallforschung Berlin (CSB), Charité - Universitätsmedizin Berlin, Berlin, Germany

[7]Klinik für Neurologie, Medical Park Berlin Humboldtmühle, Berlin, Germany

[8]Klinik und Hochschulambulanz für Neurologie, Charité-Universitätsmedizin Berlin, Berlin, Germany

[9]German Centre for Neurodegenerative Diseases (DZNE), Berlin, Germany

[10]German Centre for Cardiovascular Research (DZHK), Berlin, Germany

[11]ExcellenceCluster NeuroCure, Berlin, Germany

[12]Department of Diagnostic and Interventional Neuroradiology, University Medical Centre Hamburg-Eppendorf, Hamburg, Germany

[13]Department of Neurology, University Hospitals Leuven, Leuven, Belgium

[14]Department of Neurosciences Division of Experimental Neurology, KU Leuven—University of Leuven, Leuven, Belgium

[15]VIB, Centre for Brain & Disease Research, Laboratory of Neurobiology, Leuven, Belgium

[16]Institute of Neuroscience & Psychology, University of Glasgow, Glasgow, UK

[17]Department of Stroke Medicine, Université Claude Bernard Lyon 1, CREATIS CNRS UMR 5220-INSERM U1206, INSA-Lyon, Lyon, France

[18]Department of Radiology, Institut de Diagnostic per la Image (IDI), Hospital Dr Josep Trueta, Institut d'Investigació Biomèdica de Girona (IDIBGI), Girona, Spain

[19]Department of Neurology, Aarhus University Hospital, Aarhus, Denmark

[20]Stroke Division, Florey Institute of Neuroscience and Mental Health, University of Melbourne, Heidelberg, Victoria, Australia

[21]Department of Neurology, Austin Health, Heidelberg, Victoria, Australia

[22]Department of Neurology Amsterdam UMC, University of Amsterdam, Amsterdam, Netherlands

Correspondence
Eckhard Schlemm, UKE, Neurologie, Martinistr. 52, D-20251 Hamburg, Germany.
Email: e.schlemm@uke.de

Funding information
SPP 2041 Computational Connectomics, Grant/Award Number: Ge 844/5-1; BMBF; German Ministry for Education and Research; DFG, German Research Foundation, Grant/Award Numbers: 178316478, EXC-2049-390688087; European Union Seventh Framework Program, Grant/Award Number: 278276

Abstract

The symptoms of acute ischemic stroke can be attributed to disruption of the brain network architecture. Systemic thrombolysis is an effective treatment that preserves structural connectivity in the first days after the event. Its effect on the evolution of global network organisation is, however, not well understood. We present a secondary analysis of 269 patients from the randomized WAKE-UP trial, comparing 127 imaging-selected patients treated with alteplase with 142 controls who received placebo. We used indirect network mapping to quantify the impact of ischemic lesions on structural brain network organisation in terms of both global parameters of segregation and integration, and local disruption of individual connections. Network damage was estimated before randomization and again 22 to 36 h after administration of either alteplase or placebo. Evolution of structural network organisation was characterised by a loss in integration and gain in segregation, and this trajectory was attenuated by the administration of alteplase. Preserved brain network organization was associated with excellent functional outcome. Furthermore, the protective effect of alteplase was spatio-topologically nonuniform, concentrating on a subnetwork of high centrality supported in the salvageable white matter surrounding the ischemic cores. This interplay between the location of the lesion, the pathophysiology of the ischemic penumbra, and the spatial embedding of the brain network explains the observed potential of thrombolysis to attenuate topological network damage early after stroke. Our findings might, in the future, lead to new brain network-informed imaging biomarkers and improved prognostication in ischemic stroke.

KEYWORDS
ischemic stroke, network neuroscience, structural connectivity, systemic thrombolysis

1 | INTRODUCTION

Ischemic stroke is a leading cause of adult disability. With a global incidence of 13.7 million in 2016 it is responsible for the annual loss of 116.5 million healthy life years (Johnson et al., 2019). The associated neurological and functional deficits are caused by the tissue damage following an acute loss of blood flow to parts of the brain.

The size of an infarct is an important, yet imperfect, determinant of the severity of stroke symptoms in the acute phase and the potential for recovery (Laredo et al., 2018; Payabvash et al., 2017). The location of the infarct, in particular the involvement of eloquent cortical areas, is associated with specific clinical stroke syndromes and deficits (Cheng et al., 2014; Rothwell, 2002). Beyond these volume-dependent and local effects, ischemic lesions in strategic positions affect fibre tracts and have remote effects on the brain network structure and function (Feeney & Baron, 1986). The focal damage caused by localised ischemic infarcts alters the global topological properties of the cerebral connectome with volume-dependent increases in segregation parameters and loss of long-range integration seen in both cross-sectional (Cheng et al., 2019) and longitudinal (Pallast et al., 2020; Schlemm et al., 2020) studies. Functionally, infarcts disrupt the global organisation of synchronised neuronal activity across the brain (Griffis et al., 2019; Griffis et al., 2020) and lead to deficits in distributed processing underlying memory (Ferguson et al., 2019), consciousness (Snider et al., 2020) and speech (Yourganov et al., 2016).

Intravenous thrombolysis with recombinant tissue-plasminogen activator (rtPA) is a safe and effective treatment for acute ischemic stroke (Berge et al., 2021; Powers et al., 2015). By upregulating the intrinsic fibrinolytic pathways, it promotes the recanalization of occluded arteries and the reperfusion of ischemic tissue (Bivard et al., 2013). Early administration of rtPA reduces neurological deficits and increases the odds of achieving functional independence after stroke (Hacke et al., 2008; The National Institute of Neurological Disorders and Stroke rt-PA Stroke Study Group et al., 1995). Structurally, thrombolysis can impede the progression from poor perfusion to complete infarction (Kawano et al., 2017), and lead to smaller final infarct volumes (Mair et al., 2018). In a recent analysis of data from a large prospective, randomized, multicentre trial of thrombolysis in acute ischemic stroke (WAKE-UP) (Thomalla et al., 2018), rtPA was

associated with the preservation of structural connectivity after anterior circulation stroke, which mediated 22% of its beneficial effect on functional outcome (Schlemm et al., 2021). This study used indirect lesion network mapping to estimate lesion-induced connectivity deficits aggregated at the level of individual brain regions and quantified the causal contribution of preserved connectivity to excellent functional outcome with the main aim of better understanding the structural mechanisms underlying the clinical efficacy of thrombolysis. Previous work has not addressed the connectivity-preserving effects of thrombolysis on individual connections, their spatio-topological determinants, or their consequences for global measures of brain network integration and segregation.

In the present study, we used data from the clinical WAKE-UP trial to investigate the effect of thrombolysis on the topological structure of the cerebral structural connectome in a lesion network mapping paradigm. Based on the effect of thrombolysis on lesion growth (Mair et al., 2018), known associations between lesion volume and altered brain network topography (Cheng et al., 2019), and the natural time course of stroke-induced network disruption (Schlemm et al., 2020), we hypothesized that rtPA would prevent stroke-induced changes in the global network architecture, and be associated with a less pronounced increase in segregation parameters and a reduced loss in long-range integration. In addition, we aimed to localise the site of preserved structural connectivity underlying this protective effect, hypothesizing that it would occur predominantly at the periphery of the initial ischemic lesions, where brain tissue is acutely hypoperfused, but not irreversibly damaged.

2 | MATERIALS AND METHODS

2.1 | Study design

The WAKE-UP trial (NCT01525290) was an international, double-blind, placebo-controlled randomized clinical trial of the efficacy and safety of systemic thrombolysis with alteplase in acute ischemic stroke patients with unknown time of symptom onset (Thomalla et al., 2018). Key inclusion criterion was demonstration, on MR imaging, of an acute ischemic lesion in diffusion-weighted imaging (DWI) without established hyperintensity in fluid-attenuated inversion recovery (FLAIR). The WAKE-UP trial provided evidence that thrombolysis is effective and safe in MR imaging-selected patients with unknown symptom onset based on a DWI-FLAIR mismatch.

For this post-hoc secondary analysis, imaging and clinical data of all randomized patients were reviewed. We included patients with isolated anterior-circulation stroke who received DWI and FLAIR imaging both prior to and 22 to 36 h after randomization. Data from patients with bilateral stroke, as well as imaging data of insufficient quality, that is, those exhibiting large motion artefacts, preventing accurate segmentation and registration of stroke lesions, were excluded. Written informed consent by either patients or their legal representatives was provided according to relevant regulations. The trial was approved by local competent authorities and ethics committees at each study site. The WAKE-UP study protocol and main clinical results were published previously (Thomalla et al., 2018).

2.2 | Imaging data processing

Stroke lesions were segmented based on DWI data using a software developed for the WAKE-UP trial (Stroke Quantification Tool, SONIA) as described previously (Cheng, Boutitie, et al., 2020; Forkert et al., 2014). In summary, individual DWI and FLAIR datasets were rigidly co-registered. Apparent diffusion coefficient (ADC) maps were calculated based on two DWI datasets with *b*-values of 0 s/mm^2 and between 500 and 1500 s/mm^2 according to the imaging protocol of the study site. Stroke lesions were segmented on ADC maps using a semi-automated procedure with initial manual delineation and secondary automated refinement based on an ADC threshold of 620×10^{-6} mm^2/s. Images were visually checked for quality and plausibility of segmentation results by cross-modal inspection of FLAIR and ADC maps and manually corrected, if necessary. Lesion volumes were calculated based on final lesion segmentations in native space. Binary lesion masks were transformed to MNI (Montreal Neurological Institute) standard space by applying linear and nonlinear registrations (Fonov et al., 2009; Jenkinson et al., 2012).

2.3 | Quantification of structural network disruption

We quantified disruption of structural brain networks by mapping stroke lesion masks in MNI space onto a set of pre-defined, weighted structural reference tractograms obtained from diffusion tensor imaging (DTI) and DTI tractography in 73 healthy participants using the Network Modification (NeMo) toolbox for Matlab (Kuceyeski et al., 2013; MATLAB, 2021). The NeMo tool has previously been applied to investigate lesion-dysfunction relationships (Kuceyeski et al., 2015), white- and grey matter pathologies in normal aging (Glodzik et al., 2014), as well as prediction of clinical outcome 6 months after stroke (Kuceyeski et al., 2016). Specifically, streamlines running through the ischemic lesion were removed from the reference tractograms, resulting, for each patient, in a set of 73 lesioned tractograms. A brain parcellation based on the Desikan–Killiany cortical atlas (Desikan et al., 2006) augmented by seven subcortical regions (Supplementary Table 1) was used to convert tractograms into networks with 86 regions (defined as nodes) by counting the number of streamlines connecting any given pair of brain regions (defined as edges). Ipsilesional intra-hemispheric networks were defined as subnetworks induced by the 43 brain regions on the side of the ischemic lesion. Their global topology was characterized by graph-theoretical analysis. We chose the measure of global efficiency, that is, the average inverse shortest path length, as a marker commonly applied to infer network integration as well as the average clustering coefficient as a marker for network segregation (Rubinov & Sporns, 2010). Streamline counts of individual connections as well as the global graph

measures of each lesioned network were divided by corresponding streamline counts and null graph measures of the networks obtained from intact tractograms and averaged across the reference set. Reported connectivity strengths and network measures for stroke patients are thus relative to reference values in the healthy population ($n = 73$) included in the NeMo software.

In addition to global metrics of structural network topology, we aimed to localise potential effects of thrombolysis by studying the change of structural connectivity of individual edges from before to 22 to 36 h after randomization in WAKE-UP. In order to address the multiple testing problem inherent in mass univariate approaches of testing all edges in the structural connectome, the network-based statistic (NBS) approach was used to identify subnetworks of alteplase-responsive edges, in which progressive loss of connectivity was reduced in the alteplase group compared with placebo. The NBS methodology has been validated previously to identify connections that are associated with an experimental effect or a between-group difference (Zalesky et al., 2010).

2.4 | Interplay between lesion location, network topology and preserved connectivity

We aimed to establish a link between localised effects of alteplase on structural connectivity and overall network topology, specifically global efficiency as a marker of network integration. We therefore asked whether alteplase-responsive connections were particularly relevant to the network's integrative capacity. As an important measure for the topological importance of an individual edge in a network, we chose to study its betweenness centrality which quantifies the fraction of shortest paths between all nodes of the connectome that pass through that edge (Rubinov & Sporns, 2010). Damage to network edges with high betweenness centrality is known to result in more extensive changes of the global efficiency compared with damage to edges with relatively low centrality (Reijmer et al., 2016). Since most connections in modular networks do not support any shortest paths, we restricted analysis to so-called *backbone* edges with positive betweenness centrality in the reference network obtained from taking the median of the 73 control connectomes included in the NeMo toolbox. The importance of the subnetworks of alteplase-responsive edges as a whole was quantified by its information centrality (Latora & Marchiori, 2007), that is, the relative reduction in global efficiency of the reference network when the alteplase-responsive edges are removed.

Finally, we investigated spatio-topological predictors for the connectivity-preserving effects of alteplase. We hypothesized that the connectivity-preserving effect of treatment would be largest at the periphery of the initial lesions where brain tissue is hypoperfused, but not yet irreversibly damaged and thus potentially salvageable by reperfusion (Heiss, 2000). At the network edge level, this notion was operationalised as the average degree of disconnection induced by the initial DWI lesion before randomisation. We expected to see an inverted *U*-shaped relation with the largest treatment effects at edges with intermediate disconnection and smaller treatment effects at edges with a very high or low baseline disconnection. This would reflect the idea that fibre tracts that either run through the core of the infarct or are supported entirely in remote areas of the brain receive little benefit from connectivity-preserving treatment.

2.5 | Clinical data

Patient sex, age at symptom onset, National Institutes of Health Stroke Scale (NIHSS) score at presentation and functional outcome 90 days after stroke as well as treatment allocation to alteplase or placebo were collected from the WAKE-UP trial database. The clinical endpoint of excellent outcome (Saver et al., 2021) was defined following the primary efficacy endpoint of the WAKE-UP trial as a score of 0 or 1 point on the modified Rankin Scale (mRS) of neurologic disability (ranging from 0 [no symptoms] to 6 [death]), assessed 90 days after stroke.

2.6 | Statistical analysis

Baseline characteristics, including sex, age, NIHSS score and DWI lesion volume before randomization, were compared between patients assigned to treatment with placebo and alteplase using a two-sample *T* test and Mann–Whitney *U* test, respectively.

The association between lesion volume and global network parameters efficiency and clustering was quantified by mixed-effects linear regression. The effect of treatment allocation on evolution of network topology was assessed by comparing the within-subject changes of global efficiency and clustering between placebo and alteplase groups, controlling for both initial lesion volume and infarct growth. Sensitivity analyses included baseline-adjusted simple regression analyses of postrandomisation network measures as well as mixed-effects regressions to model longitudinal trajectories.

Logistic regression was used to associate changes in network topology with the probability of achieving an excellent clinical outcome. This analysis of functional outcome was adjusted for the stratification variables baseline NIHSS score and patient age, as well as DWI lesion volume.

The effect of alteplase on the evolution of structural connectivity at the highest possible spatial resolution was investigated by a mass-univariate linear regression analysis, in which the within-subject change in connectivity strength at each edge was modelled as a linear function of treatment, with both lesion volume and infarct growth included as nuisance regressors. The statistical model used at the edge level was thus identical to the model used in the analysis of global network parameters. Based on the result of these mass-univariate models, the distribution of the *T* statistic associated to the effect of treatment (alteplase or placebo) under the null hypothesis of no treatment effect was derived via a permutation approach based on

resampling the observed residuals of the reduced model not containing the treatment term (Freedman & Lane, 1983). Based on the observed T statistic for the treatment effect exceeding a sequence of pre-specified thresholds ranging from $t = 1.0$ to $t = 2.5$, corresponding, via the central T distribution with 269-3-1 = 265 degrees of freedom, to edge-wise mass-univariate significance levels ranging from $\alpha = 0.159$ to $\alpha = 0.0065$, progressively conservative subsets of alteplase-responsive edges were identified and grouped into connected sub-networks. Lastly, family-wise error rates of thusly formed subnetworks were quantified by relating the number of constituent edges to the null distribution of subnetwork sizes obtained from 10,000 random permutations of the original data.

To better understand the spatio-topological nonuniformity of the effect of thrombolytic treatment, we investigated the relation between alteplase-associated reduced loss of connectivity and edge betweenness centrality. Generalised linear regression analyses were used to quantify the association between the T statistic of the treatment term in the edge-level model of connectivity change and betweenness centrality for edges in the backbone of the reference network. Information centralities of NBS-identified subnetworks of alteplase-responsive edges were compared against the null distribution of information centralities of random subnetworks with the same number of edges and nodes. The latter were chosen uniformly by rejection sampling, that is, by uniformly selecting the appropriate number of edges from the reference network and accepting the sample if and only if it formed exactly one connected component and contained the desired number of nodes.

To further test the hypothesis that the connectivity-preserving effect of alteplase is largest at the periphery of the initial lesion we fitted, using least-squares, a second-degree polynomial in the initial average disconnection of an edge to model the connectivity-preserving effect of alteplase at that edge.

Network analyses were performed in MATLAB R2021a (MATLAB, 2021), statistical analyses in the R Statistical Computing Environment (version 4.0.5) (Team R Development Core, 2018).

3 | RESULTS

3.1 | Patient characteristics

Application of inclusion and exclusion criteria to arrive at the final study population is visualized in Supplementary Figure 1. Of 503 patients randomized in the WAKEUP trial to receive placebo or alteplase, 352 had MR imaging data of acceptable quality both before randomization and 22 to 36 h after stroke. Of those, 278 (79.0%) had an anterior-circulation stroke (160 lesions in the left hemisphere, 109 lesions in the right hemisphere, nine bilateral) and 269 were included in our analysis. The spatial distribution of stroke lesions at baseline is shown in Figure 1. Lesion maps stratified by treatment allocation and time point can be found as Supplementary Figure 2.

Of the 269 patients, 142 were randomized to placebo and 127 to alteplase. Their demographic and clinical characteristics are shown in Table 1. Age (placebo: mean 66.0 ± 11.1 years; alteplase: mean 65.2 ± 11.3 years) was comparable between the two groups, while baseline NIHSS scores (placebo: median 7, interquartile range [4, 11]; alteplase: median 6, IQR [3.5, 8]) was slightly higher in the placebo group.

Of the 151 patients excluded from analysis because of insufficient image quality, 119 had anterior circulation infarcts. Their age (66.4 ± 11.7 years) and baseline NIHSS scores (median 6, IQR [4, 10.5]) were similar to the study population.

3.2 | Change of global network topology

Connectivity measures were successfully calculated for all patients from lesioned reference connectomes of 73 healthy participants. In ipsilesional intrahemispheric brain networks, global network measures were linearly related to the size of the lesion (Figure 2). Specifically, pooled across time points, a 10 ml larger lesion volume was associated with 3.7 percentage points (pp) ($CI_{95\%}$ [3.9, 3.5] pp, $p < 0.0001$) smaller ipsilesional intrahemispheric global efficiency, and 3.5 pp ($CI_{95\%}$

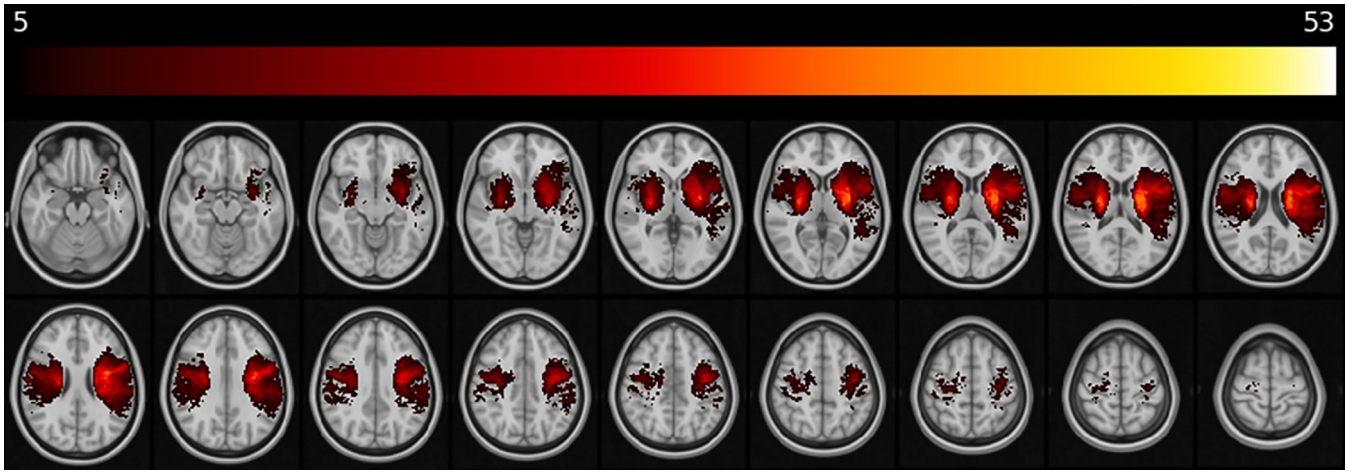

FIGURE 1 Overlay of 269 anterior-circulation stroke lesions included in the analysis. Stroke lesions have been segmented from pre-randomisation diffusion-weighted MR imaging and registered to MNI152 space. Voxels that are affected by at least five infarcts are marked.

TABLE 1 Demographic and clinical characteristics of the study population

	Whole sample $n = 269$	Placebo group $n = 142$	Alteplase group $n = 127$
Age (y)—mean (SD)	65.6 (11.2)	66.0 (11.1)	65.2 (11.3)
Female sex—*n* (%)	89 (34)	48 (34)	41 (33)
Baseline NIHSS—median (IQR)	6 (4–10)	7 (4–11)	6 (3.5–8)
Left-sided infarct—*n* (%)	160 (60)	86 (61)	74 (59)
Baseline lesion volume (ml)—median (IQR)	3.0 (1.0–9.9)	4.0 (1.3–10.2)	2.2 (0.87–9.9)
Lesion growth (ml)—median (IQR)	1.5 (0.04–9.8)	2.3 (0.24–17)	1.0 (−0.27–7.5)

Note: Measures of central tendency (mean; median) and, where applicable, dispersion (SD, standard deviation; IQR, inter-quartile range) are given for both the full sample and strata defined by randomised treatment allocation to Placebo or Alteplase. Lesion growth is measured from before to 22–36 h after randomisation.

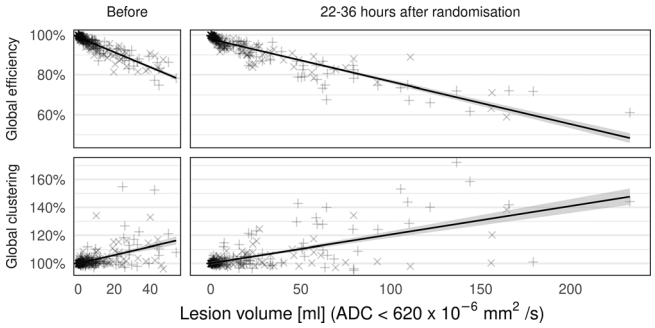

FIGURE 2 Linear association between infarct size and ipsilesional intrahemispheric global network measures. Efficiency (integration) and clustering (segregation) before and 22–36 h after randomisation (same $n = 269$ independent patients in each panel) are given relative to their average value in a set of 73 unlesioned reference connectomes. Shape indicates allocation to placebo (+) and alteplase (×). Solid lines represent estimates of conditional population averages, grey ribbons approximate 95%-confidence intervals.

[3.1, 3.9] pp, $p < 0.0001$) higher ipsilesional intrahemispheric global clustering.

Controlling for this effect of lesion volume, network measures were comparable in the placebo and alteplase groups before randomisation.

Analysis of within-subject trajectories of global network measures over the 22 to 36 h after stroke is shown in Figure 3. There was a less pronounced loss of ipsilesional global efficiency of (mean ± S.E.: −1.37 ± 0.37) pp in the alteplase group versus (−2.96 ± 0.46) pp in the placebo group, corresponding to a treatment effect of alteplase of 1.59 pp ($CI_{95\%}$ [0.42, 2.77] pp, p 0.0082). There was also a significantly attenuated increase in global clustering (alteplase: [0.14 ± 0.38] pp vs. placebo: (3.33 ± 0.76) pp), corresponding to a treatment effect of alteplase of −3.19 pp ($CI_{95\%}$ [−4.93, −1.44], p 0.0004). After adjustment for the outcome predictor pre-randomization DWI lesion volume and the potential mediator lesion growth, treatment effects were 0.59 pp ($CI_{95\%}$ [0.038, 1.14] pp, p_{adj} 0.0361) and −2.34 pp ($CI_{95\%}$ [−3.85, −0.82] pp, p_{adj} 0.0026), respectively. Similar results were obtained when network measures after randomisation were adjusted for baseline values and in a mixed-effects analysis (Supplement Table 2).

After adjustment for treatment allocation, baseline lesion volume, NIHSS score and patient age, change in graph parameters was an independent predictor of excellent clinical outcome: the probability of not achieving a score of 0 or 1 on the modified Rankin scale after 90 days was independently associated with a smaller decrease of global efficiency (adjusted odds ratio 0.88/1 pp, $CI_{95\%}$ [0.78, 0.97], p 0.0139) and a higher increase of global clustering (aOR 1.09/1 pp, $CI_{95\%}$ [1.02, 1.18], p 0.0319) over the first 22 to 36 h after stroke. When analyses were additionally adjusted for lesion growth, odds ratios were numerically similar (efficiency: aOR 0.92/1 pp, $CI_{95\%}$ [0.80, 1.03]; clustering: 1.06, [1.00, 1.16]).

3.3 | Localisation of structural network changes

Mass-univariate effects of alteplase on progression of loss of structural connectivity at individual edges across the ipsilesional brain network adjusted for baseline lesion volume and infarct growth are shown in Supplementary Figure 3. After thresholding individual treatment effects and collecting edges into connected components, network-based statistics identified subnetworks of edges exhibiting less pronounced within-subject loss of connectivity in the alteplase group compared with the placebo group. Over thresholds ranging from $t = 1.0$ to $t = 2.1$, corresponding to edge-wise mass-univariate significance levels ranging from $\alpha = 0.159$ to $\alpha = 0.0184$, subnetworks consisting of 146 ($t = 1.0$) to 15 ($t = 2.1$) edges were identified (family wise error rate <0.05; Figure 4a). Most consistently and up to the most conservative threshold of $t = 2.1$, the network-based statistics approach localised the connectivity-preserving effect of alteplase to long-range cortico-cortical connections between frontal and parietal brain areas as well as limbic regions (Figure 4b,c).

Edge-betweenness centrality scores in the intrahemispheric median reference network generated from 73 healthy subjects in the NeMo toolbox were positive in 76 of 903 (8.4%) connections (Figure 5a). Generalized regression analysis showed that for edges in this backbone, a higher betweenness centrality was associated with a stronger protective effect of alteplase treatment (p 0.0199, Figure 5b). The topological importance of the subnetworks of alteplase-responsive edges was quantified by their information

	Δ_{GGP} [pp] (Placebo)	Δ_{GGP} [pp] (Alteplase)	P	P_{adj}
Efficiency	-2.96	-1.37	0.0082	0.0361
Clustering	3.33	0.14	0.0004	0.0026

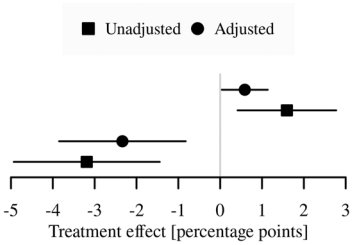

FIGURE 3 Modelling change Δ_{GGP} in the ipsilesional intrahemispheric global network measures from before to 22–36 h after randomisation as a function of treatment allocation. (Left) Temporal differences (post- minus pre-randomization) in global efficiency and clustering in the placebo and alteplase groups. Two-sided *p* values for the treatment effect of alteplase, expressed as the group difference (alteplase minus placebo), were obtained from simple or multiple linear regressions. In adjusted analyses, the possible confounders pre-randomization DWI lesion volume and lesion growth were included in the linear model as nuisance regressors. (Right) Point estimates (■,●) and 95% confidence intervals (——) of the effect of alteplase are represented as boxes and lines

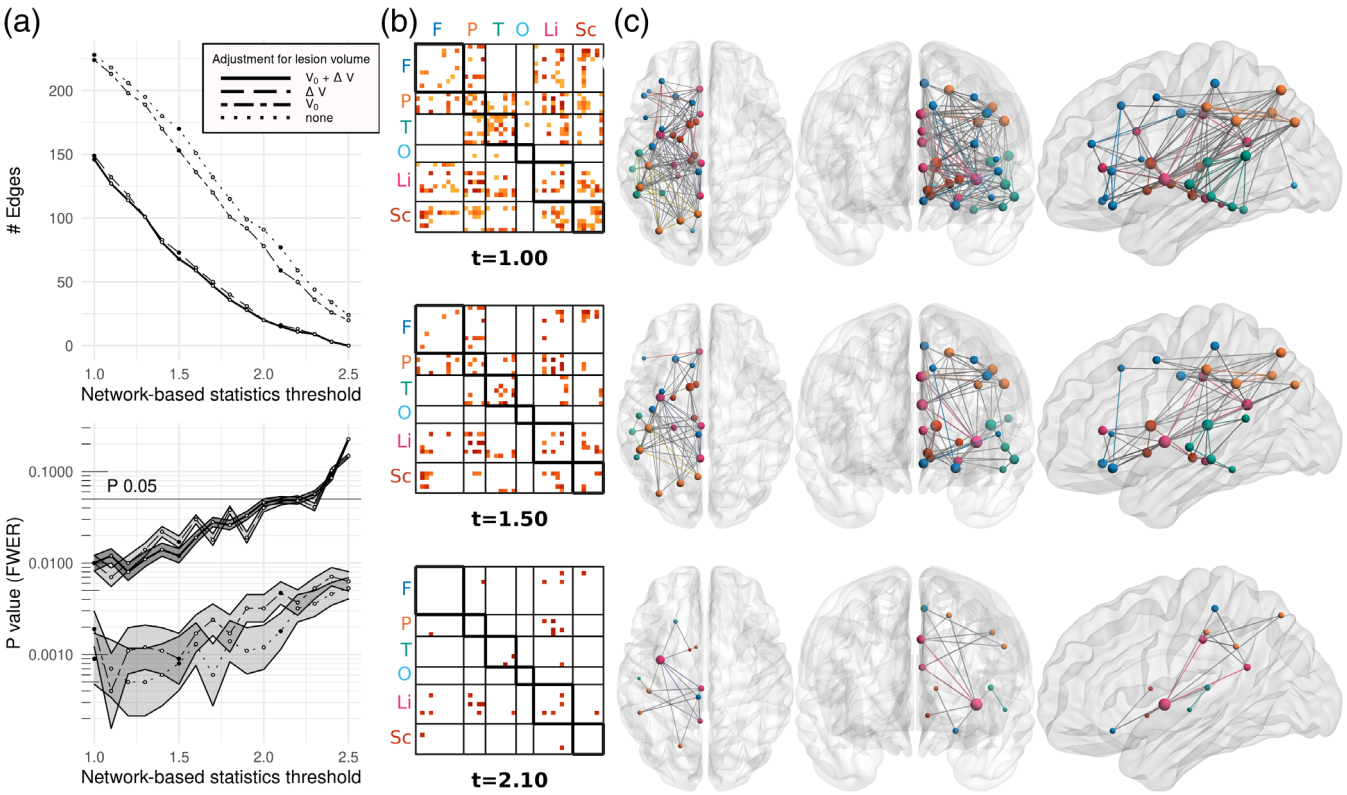

FIGURE 4 Evolution of structural connectivity after thrombolysis compared with placebo. (a) Size (top) and family-wise error rate (FWER, bottom) of the largest connected component (LCC) of the set of supra-critical edges (T statistic for treatment effect exceeding prespecified thresholds). FWERs are obtained by comparing the size of the empirical LCC to the null distribution of sizes of maximal LCC obtained from 10,000 random permutations of the empirical data. Approximate 95% confidence intervals (ribbon) of FWERs were computed using Wilson's formula (Wilson, 1927). Results from fully adjusted models with both baseline lesion volume (V_0) and infarct growth (ΔV) included as nuisance variables are shown in solid black. Results from partially adjusted and unadjusted models are shown for comparison by broken lines. (b) Weighted adjacency matrix representations of subnetworks identified for selected T thresholds under full adjustment for lesion volume. Nodes are grouped according to anatomical lobes with intralobar connections outlined along the main diagonal. Colour indicates the magnitude of the treatment effect of alteplase on preservation of connectivity, with darker red indicating higher values. (c) Balls-and-sticks models of the same subnetworks in axial, coronal and sagittal projections. The radius of the ball representing a region of the augmented Desikan–Killiany atlas is proportional to its number of connections; colour indicates membership to frontal (F, cerulean), parietal (P, sun), temporal (T, dark cyan), occipital (O, summer sky) and limbic (Li, violet red) lobes, or subcortical structures (Sc, orange)

centrality, for example, the relative decline in global efficiency that their removal would induce in the median reference brain network. Information centrality of the subnetworks of alteplase-responsive edges was significantly higher than in random null subnetworks of the same size for all *T* thresholds <1.69 (Figure 5c). While information centrality did not, then, exceed the 95% quartile of the null

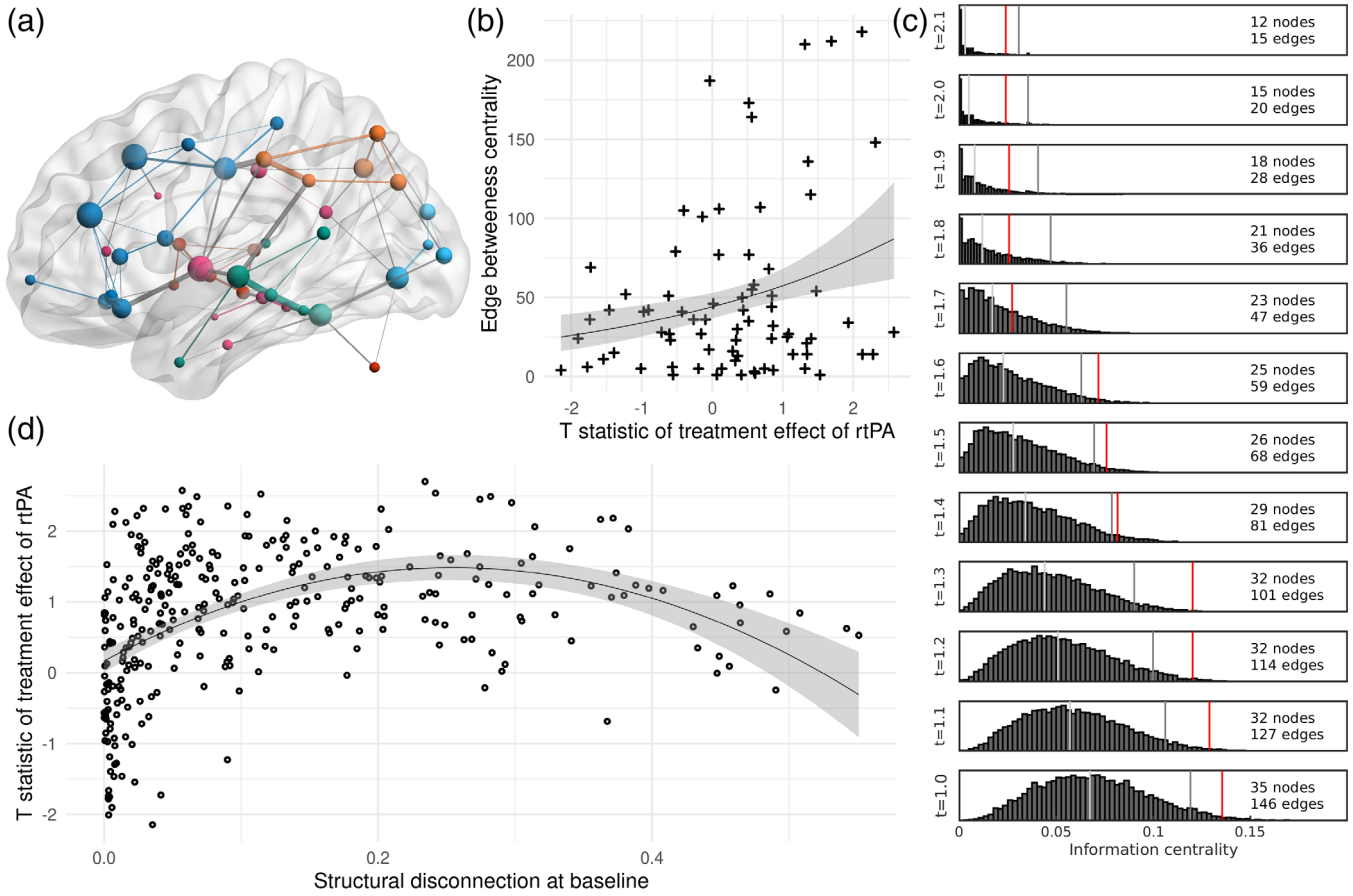

FIGURE 5 Topological profile of connectivity-preserving effect of alteplase. (a) Network backbone comprising connections of nonvanishing edge betweenness centrality (EBC). Line thickness indicates edge centrality, ball size node degree. (b) Regression analysis between betweenness centrality and effect of alteplase at individual connections of the reference network backbone, quantified by the *T* statistic of the treatment term in fully lesion volume-adjusted linear models of connectivity change. Each marker (+) represents one of 76 unique backbone edges. Positive, integer-valued EBC is modelled as a function of treatment effect using a generalized linear model with a logarithmic link function and a quasi-binomial response distribution (p 0.0199). (c) Information centrality of NBS-identified subnetworks of alteplase-responsive connections (vertical red line) in comparison to null distributions of information centrality (shown as histograms) of $n = 10{,}000$ random connected subnetworks with the same number of edges and nodes, for selected T thresholds under full adjustment for lesion volume. Vertical grey lines indicate median and 95% quantile of the null distribution. (d) Inverse *U*-shaped relation between the average degree of initial disconnection of an edge and connectivity-preserving treatment effect of alteplase, quantified as the T statistic of the treatment term in edgewise linear models of change in connectivity of individual connections adjusted for baseline lesion volume and change in lesion volume. Each marker (o) represents one of $n = 407$ edges with non-zero connectivity. The solid black line represents the least-square second-degree polynomial fit with equation $y = -0.17 + 10.4x - 20.4x^2$, the shaded ribbon formal pointwise 95% confidence intervals

distribution of centrality values in random size-matched connected networks, it was still substantially higher than the median of this distribution.

Figure 5d displays the relation between the average degree of initial disconnection of an edge and the connectivity-preserving effect of alteplase at the edge. The inverse *U*-shape (p value for nonlinearity <0.0001) shows that alteplase had the largest effect at edges that were, on average across the study sample, partially affected by the ischemic lesions at baseline with the maximal treatment effect occurring at edges with averaged disconnection of about 25%. Thrombolysis had little effect at edges whose connectivity was mildly or severely compromised initially.

4 | DISCUSSION

We investigated the impact of thrombolysis on the evolution of structural brain networks in patients with anterior-circulation stroke enrolled in the WAKE-UP trial. We used indirect lesion network mapping to transform empirical MRI-derived lesion maps into estimated network disruptions in reference connectomes from healthy participants. As our first main result, treatment with rtPA was associated with reduced stroke-related increase in structural network segregation and reduced loss in long-range network integration over the first 22 to 36 h after stroke beyond the effect of reduced lesion growth. Secondly, preservation of structural connectivity occurred

predominantly in an interlobar cortico-cortical network of high-centrality edges supported in the white matter surrounding initial ischemic lesions.

The observed patterns of stroke-induced alterations in global network architecture are consistent with previous work. Projection of ischemic lesions into reference tractograms resulted in higher segregation and lower integration parameters than in the intact connectome, with a linear relation between volume of the lesion and degree of altered topology. The distribution of lesion sizes and locations in the current study with an abundance of small subcortical infarcts is similar to a chronic stroke cohort (Cheng et al., 2019), in which the same pattern of increased clustering and reduced efficiency was observed and linked to the preferential damage of long-range connections. The almost mirror-like appearance of the volume dependence of network measures in Figure 2 is typical for a sample of anterior-circulations stroke patients (Figure 1) and might be different for more peripheral or infratentorial lesion distributions. Smaller integration and higher segregation parameters as well as changes in central network hubs as a result of focal brain damage have previously been described in animal studies using high-resolution tensor imaging and network simulations (Sinke et al., 2018; Straathof et al., 2019). In addition to reduced measures of centrality in stroke hemispheres (Lee et al., 2015), structural network studies have also revealed changes in the contralateral hemisphere, such as reduced communicability (Crofts et al., 2011) and altered backbone structure(van den Heuvel et al., 2012), after stroke.

While the patterns of network damage induced by a focal lesion are increasingly well understood, the effects of a lesion evolving over time are less clear. In our study we observed, over the first 22 to 36 h after stroke, an early increase in segregation parameters and a decline in integration parameters, which remained significant after controlling for the effect of lesion size. A similar effect, albeit at a different time scale and thus confounded by secondary processes of network degeneration, has previously been reported in a longitudinal cohort study (Schlemm et al., 2020), in which, over a one-year follow-up period, gradual changes of the global network topology in terms of global efficiency and modularity beyond the effect of the acute disruption occurred. In that study, lesion size in the acute phase was a strong, yet imperfect, predictor for subsequent progressive network degeneration. This is in contrast to our results, where infarct growth, but not baseline lesion volume, was associated with short-term network change. The integrity of white matter pathways as the substrate for global network organisation has been shown to undergo similar changes after stroke (Koch et al., 2016), with the time course of associated measures of structural connectivity mirroring those of derived network parameters (Schlemm et al., 2020).

The efficacy of acute stroke treatments is primarily assessed against clinical endpoints including neurological impairment, disability and quality of life (Saver, 2011). Imaging markers of brain perfusion and tissue state are used to supplement primary analyses and provide information on the immediate effect of an intervention (De Silva et al., 2009). Thus both vessel recanalization and slowed infarct growth have been associated with acute reperfusion treatment (Mair et al., 2018; Rha & Saver, 2007; Zangerle et al., 2007). Little information, however, is available on the effect of medical interventions on the progression of network organisation after stroke. We have previously shown that intravenous thrombolysis helps preserve structural connectivity after stroke (Schlemm et al., 2021). Extending this result, we find that the increase in clustering and the loss of efficiency in stroke patients over the first 22 to 36 h after the event is attenuated after receiving alteplase in comparison to placebo. This effect remained statistically significant after controlling for the alteplase-dependent reduction in lesion growth observed in this population (Figure 3).

Preservation of both structural connectivity (Schlemm et al., 2021) and of physiological network organisation quantified by integration and segregation parameters, as shown above, was associated with achieving an excellent functional outcome 90 days after stroke as measured in terms of activity of daily living on the modified Ranking scale. This reflects the integrity of the structural connectome as a prerequisite for normal neurological function in multiple domains, with disruptions of the connectome linked to a wide variety of acute and chronic stroke symptoms such as aphasia (Gleichgerrcht et al., 2015), motor deficits (Aerts et al., 2016), depression (Xu et al., 2019) and apathy (Tay et al., 2020). More specifically, our results are consistent with previous studies of both voxel-based and network-informed measures of lesion impact in stroke, in which the location and number of rich-club nodes affected by the lesion were used to predict functional outcome (Cheng et al., 2014; Ktena et al., 2019; Schirmer et al., 2019). Subsequent developments combined spatial and topological information by convolving hub-scores and lesion overlap in 90 brain regions and showed that the resulting lesion impact score has utility in predicting cognitive recovery after stroke (Aben et al., 2019). These results hint at a parallel between the notions of 'network hub' and 'edge centrality', in which the former emphasizes the importance of a node in the network, whereas the latter operates at the level on individual connections (Zhou et al., 2016).

Previous work revealed the largest effects of alteplase at preserving structural connectivity in the fibre bundles related to the cortical areas of the frontal, parietal and temporal lobes adjacent to the central sulcus (Schlemm et al., 2021). Here, we further increased the spatio-topological resolution of these findings and localised the protective effects of alteplase to networks of cortico-cortical connections surrounding the central region of the ipsilesional hemisphere (Figure 4c). Considering the homogenous distribution of predominantly subcortical infarcts in this population of patients with anterior-circulation stroke, the cerebral white matter supporting these alteplase-responsive networks has a large spatial overlap with the periphery of the individual initial DWI lesions, which are most vulnerable to delayed infarction due to expansion of the ischemic core (Read et al., 2000). By topologically localizing the connectivity-preserving effect of alteplase to specific edges in the connectome, our results indirectly characterise the spatial profile of local infarct progression. Further research is needed to clarify if specific patterns of spatio-topological lesion evolution are related to the loss or recovery of distinct neurological functions beyond the global disability scale used in the WAKE-UP trial.

The interplay between the location of ischemic lesions and the topology of spatially embedded brain networks helps explain the changes in global network organisation observed in this study. We showed that, at the population-level, the connectivity-preserving effect of alteplase is largest for connections located at the periphery of the spatial distribution of ischemic lesions (Figures 4c and 5d), and thus, by homogeneity of our sample, of individual lesions. This result is consistent with the proposition that reperfusion treatment preserves brain structure in a spatially nonuniform fashion. Indeed, its effect is expected to be highest in the ischemic penumbra, where tissue is acutely hypoperfused, but not yet critically damaged (Baron, 2018; Kawano et al., 2017). Irreversibly infarcted tissue at the core of the infarct as well as healthy brain regions far away from the site of ischemia, on the other hand, are expected to receive little benefit, from restoring perfusion. Our results imply that, in the case of predominantly subcortical anterior-circulation infarcts, salvaged brain tissue surrounding the ischemic core contains white matter fibre tracts which contribute above-average to the integrative capacity of the hemispheric brain network (Figure 5b,c). This reflects the intuition that infarcts in our study sample, often involving the basal ganglia and internal capsule, were located in a central and densely connected part of brain networks. The spatial embedding of the connectome thus mediates the topologically nonuniform efficacy of alteplase at preserving the integrity of high-centrality connections and explains the lesion volume-independent protective effect of reperfusion treatment on global network topology.

Our findings of preserved connectivity as a consequence of alteplase-induced salvage of peri-core penumbral brain tissue also provide further insight into mechanisms of delayed recovery after stroke. Beyond the immediate benefits of reduced lesion volume, the integrity of peri-infarct connections may facilitate remote compensatory changes and thus promote adaptive plasticity (Furlan et al., 1996). Similarly, these adaptive processes may benefit from and proceed more easily in the presence of undisturbed brain network topology (Dirren & Carrera, 2017).

We used an indirect lesion network mapping approach to estimate the impact of a focal ischemic lesion on the brain connectome (Kuceyeski et al., 2013). The advantages and shortcomings of this method to quantify network disruptions and infer mechanisms underlying the associated clinical deficits have been discussed at length (Boes, 2021; Boes et al., 2021; Salvalaggio et al., 2020; Umarova & Thomalla, 2020). In the case of a multi-centric acute clinical stroke trial like WAKE-UP, the following points are particularly pertinent (Schlemm et al., 2021): beyond standard MR imaging protocols used in acute ischemic stroke, indirect network mapping does not require the acquisition of high-resolution diffusion sequences, which are time-consuming, vulnerable to confounding by motion artefacts and prone to induce selection bias. Restricting analyses to use fast and robust MRI sequences is also a prerequisite for translating our findings into clinical practice and to further assess the prognostic accuracy of short term preservation of network organisation for functional outcome in a larger prospective sample. Indirect lesion network mapping is invariably limited in its ability to estimate "exofocal" network disruptions occurring outside of the lesion itself, be it via diaschisis or peri-infarct selective neuronal loss (Baron et al., 2014; Carrera et al., 2013; Carrera & Tononi, 2014; Cheng, Dietzmann, et al., 2020; Zhang et al., 2012). However, the contribution of these delayed network disruption mechanisms is likely to be minor in the timeframe up to 36 h after stroke studied here. Moreover, despite this methodological limitation, NeMo, the particular toolbox used in this study, has been shown repeatedly to produce clinically and anatomically valid estimates of structural disconnection (Kuceyeski et al., 2014, 2015, 2016; Olafson et al., 2021; Respino et al., 2019; Tozlu et al., 2021). Thus, while indirect network mapping only provides surrogate markers of true neuronal disconnection and is contingent on both the validity of the tractography algorithm performed in the underlying reference population and the assumption that lesion-induced effects exceed inter-individual variability in white matter structure, it has significant utility in situations in which subject-specific diffusion imaging, tractography and network reconstruction cannot be performed.

Our results are constrained by a number of limitations. The study population consisted of patients with mild-to-moderate anterior-circulation stroke with unknown time of symptom onset whose stroke had likely occurred within 4.5 h and who were randomized to treatment with alteplase or placebo. While the risk of selection bias due to lack of imaging data seems low, our results cannot readily be generalized to patients with more severe or posterior circulation stroke, or to the effect of late or mechanical revascularization. Also, the population underlying the reference tractograms was not age-matched to our sample of acute stroke patients. An important extension of the present work would be an analysis of the effects of thrombolysis on the trajectories of measures of brain network topology beyond 36 h. Since, in the absence of reperfusion treatment, infarcts have the potential to grow beyond 36 h (Christensen et al., 2019; Tate et al., 2021), the indirectly assessed connectivity-preserving effect of thrombolysis might then be even larger. On the other hand, it is expected that secondary processes, including peri-infarct selective neuronal loss and diaschisis, but also compensatory increases in connectivity, become more relevant. A combination of techniques is therefore necessary to accurately map changes in network organisation in the subacute phase.

In summary, our analysis shows that systemic thrombolysis after anterior-circulation stroke preserves structural connectivity at the periphery of the ischemic lesion. Preservation of topologically important connections supported by brain tissue in this area leads to an attenuation of progressive global network disruption in terms of both segregation and integration parameters, which is a predictor for excellent outcome.

ACKNOWLEDGMENTS

The WAKE-UP trial was supported by a grant (278276) from the European Union Seventh Framework Program. Dr Endres received funding from Deutsche Forschungsgemeinschaft (DFG, German Research Foundation) under Germanys Excellence Strategy-EXC-2049-390688087 and from Bundesministerium für Bildung und Forschung (BMBF; German Ministry for Education and Research) for the Centre for Stroke Research Berlin. Christian Gerloff also acknowledges funding from SPP 2041 Computational Connectomics, project Ge 844/5-1.

FUNDING INFORMATION

Work on the presented project was supported by funding from the Deutsche Forschungsgemeinschaft (DFG, German Research Foundation)—178316478—C1 (CG) & C2 (BC, GT).

CONFLICT OF INTEREST

Martin Ebinger reports receiving grants from Bayer and fees paid to the Charité from Bayer, Boehringer Ingelheim, BMS, Daiichi Sankyo, Amgen, GSK, Sanofi, Covidien, Novartis, Pfizer, all outside the submitted work. Jochen B. Fiebach, grants from European Union 7th Framework Program during the conduct of the study and personal fees from Bioclinica, Artemida, Cerevast, Brainomix, BMS, Merck, Eisai, Biogen, Guerbet, and Nicolab outside the submitted work; Ivana Galinovic, receiving a grant from European Union 7th Framework Program during the conduct of the study; Keith W. Muir, receiving advisory board fees from Boehringer Ingelheim, Bayer, Daiichi Sankyo, ReNeuron and research support from Boehringer Ingelheim; Claus Z. Simonsen, receiving research grants from Novo Nordisk Foundation and speaker fees from Bayer; Christian Gerloff, receiving honoraria as speaker or consultant from Abbott, Amgen, Bayer Vital, Bristol-Myers-Squibb, Boehringer Ingelheim, Daiichi-Sankyo, Sanofi Aventis, and Prediction Biosciences, all outside the submitted work; Götz Thomalla, receiving consulting fees from Acandis and Portola, grant support and lecture fees from Bayer, lecture fees from Boehringer Ingelheim, Bristol-Myers Squibb/Pfizer, and Daiichi Sankyo, and consulting fees and lecture fees from Stryker, all outside the submitted work. All other authors declare no competing interests.

DATA AVAILABILITY STATEMENT

Fully anonymized patient-level data sufficient to reproduce all analyses, including age, baseline NIHSS score, lesion volumes, treatment allocation, connectivity measurements, and functional outcome, are available on GitHub (https://github.com/csi-hamburg/WU-NeMo-Topology). Imaging data, after de-identification, will be shared with the Virtual International Stroke Trials Archive (VISTA) and be accessible according to the VISTA rules (http://www.virtualtrialsarchives.org/vista).

ORCID

Eckhard Schlemm https://orcid.org/0000-0002-5729-2935
Märit Jensen https://orcid.org/0000-0001-7793-0941
Amy Kuceyeski https://orcid.org/0000-0002-5050-8342
Bastian Cheng https://orcid.org/0000-0003-2434-1822

REFERENCES

Aben, H. P., Biessels, G. J., Weaver, N. A., Spikman, J. M., Visser-Meily, J. M. A., de Kort, P. L. M., Reijmer, Y. D., & Jansen, B. P. W. (2019). Extent to which network hubs are affected by ischemic stroke predicts cognitive recovery. *Stroke*, *50*, 2768–2774.

Aerts, H., Fias, W., Caeyenberghs, K., & Marinazzo, D. (2016). Brain networks under attack: Robustness properties and the impact of lesions. *Brain*, *139*, 3063–3083.

Baron, J. C. (2018). Protecting the ischaemic penumbra as an adjunct to thrombectomy for acute stroke. *Nature Reviews Neurology*, *14*, 325–337.

Baron, J. C., Yamauchi, H., Fujioka, M., & Endres, M. (2014). Selective neuronal loss in ischemic stroke and cerebrovascular disease. *Journal of Cerebral Blood Flow and Metabolism*, *34*, 2–18.

Berge E, Whiteley W, Audebert H, Marchis GM De, Fonseca AC, Padiglioni C, Ossa NP de la, Strbian D, Tsivgoulis G, Turc G (2021): European stroke organisation (ESO) guidelines on intravenous thrombolysis for acute ischaemic stroke. *European Stroke Journal 6*. https://doi.org/10.1177/2396987321989865, I, LXII.

Bivard, A., Lin, L., & Parsonsb, M. W. (2013). Review of stroke thrombolytics. *Journal of Stroke*, *15*, 90–98. https://doi.org/10.5853/jos.2013.15.2.90

Boes, A. D. (2021). Lesion network mapping: Where do we go from here? *Brain*, *144*, e5.

Boes, A. D., Salvalaggio, A., Pini, L., de Grazia, M. F., de Schotten, M. T., Zorzi, M., & Corbetta, M. (2021). Lesion network mapping: Where do we go from here? *Brain*, *144*, e6.

Carrera, E., Jones, P. S., Morris, R. S., Alawneh, J., Hong, Y. T., Aigbirhio, F. I., Fryer, T. D., Adrian Carpenter, T., Warburton, E. A., & Baron, J. C. (2013). Is neural activation within the rescued penumbra impeded by selective neuronal loss? *Brain*, *136*, 1816–1829.

Carrera, E., & Tononi, G. (2014). Diaschisis: Past, present, future. *Brain*, *137*, 2408–2422.

Cheng, B., Boutitie, F., Nickel, A., Wouters, A., Cho, T. H., Ebinger, M., Endres, M., Fiebach, J. B., Fiehler, J., Galinovic, I., Puig, J., Thijs, V., Lemmens, R., Muir, K. W., Nighoghossian, N., Pedraza, S., Simonsen, C. Z., Gerloff, C., & Thomalla, G. (2020). Quantitative signal intensity in fluid-attenuated inversion recovery and treatment effect in the WAKE-UP trial. *Stroke*, *51*, 209–215. https://doi.org/10.1161/STROKEAHA.119.027390

Cheng, B., Dietzmann, P., Schulz, R., Boenstrup, M., Krawinkel, L., Fiehler, J., Gerloff, C., & Thomalla, G. (2020). Cortical atrophy and transcallosal diaschisis following isolated subcortical stroke. *Journal of Cerebral Blood Flow and Metabolism*, *40*, 611–621.

Cheng, B., Forkert, N. D., Zavaglia, M., Hilgetag, C. C., Golsari, A., Siemonsen, S., Fiehler, J., Pedraza, S., Puig, J., Cho, T. H., Alawneh, J., Baron, J. C., Ostergaard, L., Gerloff, C., & Thomalla, G. (2014). Influence of stroke infarct location on functional outcome measured by the modified Rankin scale. *Stroke*, *45*, 1695–1702. https://doi.org/10.1161/STROKEAHA.114.005152

Cheng, B., Schlemm, E., Schulz, R., Boenstrup, M., Messé, A., Hilgetag, C., Gerloff, C., & Thomalla, G. (2019). Altered topology of large-scale structural brain networks in chronic stroke. *Brain Communications*, *1*, fcz020. https://doi.org/10.1093/braincomms/fcz020/5581344

Christensen, S., Mlynash, M., Kemp, S., Yennu, A., Heit, J. J., Marks, M. P., Lansberg, M. G., & Albers, G. W. (2019). Persistent target mismatch profile >24 hours after stroke onset in DEFUSE 3. *Stroke*, *50*, 754–757.

Crofts, J. J., Higham, D. J., Bosnell, R., Jbabdi, S., Matthews, P. M., Behrens, T. E. J., & Johansen-Berg, H. (2011). Network analysis detects changes in the contralesional hemisphere following stroke. *NeuroImage*, *54*, 161–169.

de Silva, D. A., Fink, J. N., Christensen, S., Ebinger, M., Bladin, C., Levi, C. R., Parsons, M., Butcher, K., Barber, P. A., Donnan, G. A., & Davis, S. M. (2009). Assessing reperfusion and recanalization as markers of clinical outcomes after intravenous thrombolysis in the echoplanar imaging thrombolytic evaluation trial (EPITHET). *Stroke*, *40*, 2872–2874. https://doi.org/10.1161/STROKEAHA.108.543595

Desikan, R. S., Ségonne, F., Fischl, B., Quinn, B. T., Dickerson, B. C., Blacker, D., Buckner, R. L., Dale, A. M., Maguire, R. P., Hyman, B. T., Albert, M. S., & Killiany, R. J. (2006). An automated labeling system for subdividing the human cerebral cortex on MRI scans into gyral based regions of interest. *NeuroImage*, *31*, 968–980.

Dirren, E., & Carrera, E. (2017). Resilience of brain networks after stroke. In *Neurobiological and psychological aspects of brain recovery*

(pp. 193–209). Springer, Cham. https://doi.org/10.1007/978-3-319-52067-4_10

Feeney, D. M., & Baron, J. C. (1986). Diaschisis. *Stroke*, *17*, 817–830.

Ferguson, M. A., Lim, C., Cooke, D., Darby, R. R., Wu, O., Rost, N. S., Corbetta, M., Grafman, J., & Fox, M. D. (2019). A human memory circuit derived from brain lesions causing amnesia. *Nature Communications*, *10*, 1–9.

Fonov, V., Evans, A., McKinstry, R., Almli, C., & Collins, D. (2009). Unbiased nonlinear average age-appropriate brain templates from birth to adulthood. *NeuroImage*, *47*, S102.

Forkert, N. D., Cheng, B., Kemmling, A., Thomalla, G., & Fiehler, J. (2014). ANTONIA perfusion and stroke: A software tool for the multi-purpose analysis of MR perfusion-weighted datasets and quantitative ischemic stroke assessment. *Methods of Information in Medicine*, *53*, 469–481.

Freedman, D., & Lane, D. (1983). A nonstochastic interpretation of reported significance levels. *Journal of Business & Economic Statistics*, *1*, 292.

Furlan, M., Marchai, G., Viader, F., Derlon, J. M., & Baron, J. C. (1996). Spontaneous neurological recovery after stroke and the fate of the ischemic penumbra. *Annals of Neurology*, *40*, 216–226.

Gleichgerrcht, E., Kocher, M., Nesland, T., Rorden, C., Fridriksson, J., & Bonilha, L. (2015). Preservation of structural brain network hubs is associated with less severe post-stroke aphasia. *Restorative Neurology and Neuroscience*, *34*, 19–28.

Glodzik, L., Kuceyeski, A., Rusinek, H., Tsui, W., Mosconi, L., Li, Y., Osorio, R. S., Williams, S., Randall, C., Spector, N., McHugh, P., Murray, J., Pirraglia, E., Vallabhajosula, S., Raj, A., & de Leon, M. J. (2014). Reduced glucose uptake and Aβ in brain regions with hyperintensities in connected white matter. *NeuroImage*, *100*, 684–691.

Griffis, J. C., Metcalf, N. V., Corbetta, M., & Shulman, G. L. (2019). Structural disconnections explain brain network dysfunction after stroke. *Cell Reports*, *28*, 2527–2540.e9.

Griffis, J. C., Metcalf, N. V., Corbetta, M., & Shulman, G. L. (2020). Damage to the shortest structural paths between brain regions is associated with disruptions of resting-state functional connectivity after stroke. *NeuroImage*, *210*, 116589.

Hacke, W., Kaste, M., Bluhmki, E., Brozman, M., Dávalos, A., Guidetti, D., Larrue, V., Lees, K. R., Medeghri, Z., Machnig, T., Schneider, D., von Kummer, R., Wahlgren, N., & Toni, D. (2008). Thrombolysis with Alteplase 3 to 4.5 hours after acute ischemic stroke. *The New England Journal of Medicine*, *359*, 1317–1329. https://doi.org/10.1056/NEJMoa0804656

Heiss, W. D. (2000). Ischemic penumbra: Evidence from functional imaging in man. *Journal of Cerebral Blood Flow and Metabolism*, *20*, 1276–1293. https://doi.org/10.1097/00004647-200009000-00002

Jenkinson, M., Beckmann, C. F., Behrens, T. E. J., Woolrich, M. W., & Smith, S. M. (2012). Review FSL. *NeuroImage*, *62*, 782–790.

Johnson, C. O., Nguyen, M., Roth, G. A., Nichols, E., Alam, T., Abate, D., Abd-Allah, F., Abdelalim, A., Abraha, H. N., Abu-Rmeileh, N. M., Adebayo, O. M., Adeoye, A. M., Agarwal, G., Agrawal, S., Aichour, A. N., Aichour, I., Aichour, M. T. E., Alahdab, F., Ali, R., … Murray, C. J. L. (2019). Global, regional, and national burden of stroke, 1990–2016: A systematic analysis for the global burden of disease study 2016. *Lancet Neurology*, *18*, 439–458.

Kawano, H., Bivard, A., Lin, L., Ma, H., Cheng, X., Aviv, R., O'Brien, B., Butcher, K., Lou, M., Zhang, J., Jannes, J., Dong, Q., Levi, C. R., & Parsons, M. W. (2017). Perfusion computed tomography in patients with stroke thrombolysis. *Brain*, *140*, 684–691.

Koch, P., Schulz, R., & Hummel, F. C. (2016). Structural connectivity analyses in motor recovery research after stroke. *Annals of Clinical Translational Neurology*, *3*, 233–244. https://doi.org/10.1002/acn3.278

Ktena, S. I., Schirmer, M. D., Etherton, M. R., Giese, A.-K. K., Tuozzo, C., Mills, B. B., Rueckert, D., Wu, O., & Rost, N. S. (2019). Brain connectivity measures improve modeling of functional outcome after acute ischemic stroke. *Stroke*, *50*, 2761–2767. https://doi.org/10.1161/STROKEAHA.119.025738

Kuceyeski, A., Kamel, H., Navi, B. B., Raj, A., & Iadecola, C. (2014). Predicting future brain tissue loss from white matter connectivity disruption in ischemic stroke. *Stroke*, *45*, 717–722.

Kuceyeski, A., Maruta, J., Relkin, N., & Raj, A. (2013). The network modification (NeMo) tool: Elucidating the effect of white matter integrity changes on cortical and subcortical structural connectivity. *Brain Connectivity*, *3*, 451–463.

Kuceyeski, A., Navi, B. B., Kamel, H., Raj, A., Relkin, N., Toglia, J., Iadecola, C., & O'Dell, M. (2016). Structural connectome disruption at baseline predicts 6-months post-stroke outcome. *Human Brain Mapping*, *37*, 2587–2601.

Kuceyeski, A., Navi, B. B., Kamel, H., Relkin, N., Villanueva, M., Raj, A., Toglia, J., O'Dell, M., & Iadecola, C. (2015). Exploring the brain's structural connectome: A quantitative stroke lesion-dysfunction mapping study. *Human Brain Mapping*, *36*, 2147–2160.

Laredo, C., Zhao, Y., Rudilosso, S., Renú, A., Pariente, J. C., Chamorro, Á., & Urra, X. (2018). Prognostic significance of infarct size and location: The case of insular stroke. *Scientific Reports*, *8*, 9498.

Latora, V., & Marchiori, M. (2007). A measure of centrality based on network efficiency. *New Journal of Physics*, *9*, 188. https://doi.org/10.1088/1367-2630/9/6/188

Lee, M. H., Shin, Y., Lee, S. H., Cha, Y. J., Kim, D. Y., Han, B. S., & You, S. H. (2015). Diffusion tensor imaging to determine the potential motor network connectivity between the involved and non-involved hemispheres in stroke. *Bio-medical Materials and Engineering*, *26*, S1447–S1453. https://doi.org/10.3233/BME-151443

Mair, G., Von Kummer, R., Morris, Z., Von Heijne, A., Bradey, N., Cala, L., Peeters, A., Farrall, A. J., Adami, A., Potter, G., Sandercock, P. A. G., Lindley, R. I., & Wardlaw, J. M. (2018). Effect of IV alteplase on the ischemic brain lesion at 24-48 hours after ischemic stroke. *Neurology*, *91*, E2067–E2077.

MATLAB (2021): R2021a (9.2.0.556344). The MathWorks Inc.

Olafson, E. R., Jamison, K. W., Sweeney, E. M., Liu, H., Wang, D., Bruss, J. E., Boes, A. D., & Kuceyeski, A. (2021). Functional connectome reorganization relates to post-stroke motor recovery and structural and functional disconnection. *NeuroImage*, *245*, 118642.

Pallast, N., Wieters, F., Nill, M., Fink, G. R., & Aswendt, M. (2020). Graph theoretical quantification of white matter reorganization after cortical stroke in mice. *NeuroImage*, *217*, 116873.

Payabvash, S., Taleb, S., Benson, J. C., & McKinney, A. M. (2017). Acute ischemic stroke infarct topology: Association with lesion volume and severity of symptoms at admission and discharge. *American Journal of Neuroradiology*, *38*, 58–63.

Powers, W. J., Derdeyn, C. P., Biller, J., Coffey, C. S., Hoh, B. L., Jauch, E. C., Johnston, K. C., Johnston, S. C., Khalessi, A. A., Kidwell, C. S., Meschia, J. F., Ovbiagele, B., & Yavagal, D. R. (2015). 2015 American Heart Association/American stroke association focused update of the 2013 guidelines for the early management of patients with acute ischemic stroke regarding endovascular treatment: A guideline for healthcare professionals from the American. *Stroke*, *46*, 3020–3035.

Read, S. J., Hirano, T., Abbott, D. F., Markus, R., Sachinidis, J. I., Tochon-Danguy, H. J., Chan, J. G., Egan, G. F., Scott, A. M., Bladin, C. F., McKay, W. J., & Donnan, G. A. (2000). The fate of hypoxic tissue on 18F-fluoromisonidazole positron emission tomography after ischemic stroke. *Annals of Neurology*, *48*, 228–235.

Reijmer, Y. D., Fotiadis, P., Piantoni, G., Boulouis, G., Kelly, K. E., Gurol, M. E., Leemans, A., O'Sullivan, M. J., Greenberg, S. M., & Viswanathan, A. (2016). Small vessel disease and cognitive impairment: The relevance of central network connections. *Human Brain Mapping*, *37*, 2446–2454.

Respino, M., Jaywant, A., Kuceyeski, A., Victoria, L. W., Hoptman, M. J., Scult, M. A., Sankin, L., Pimontel, M., Liston, C., Belvederi Murri, M., Alexopoulos, G. S., & Gunning, F. M. (2019). The impact of white matter hyperintensities on the structural connectome in late-life

depression: Relationship to executive functions. *NeuroImage: Clinical*, *23*, 101852.
Rha, J. H., & Saver, J. L. (2007). The impact of recanalization on ischemic stroke outcome: A meta-analysis. *Stroke*, *38*, 967–973.
Rothwell, P. (2002). Stroke syndromes, 2nd edn, and uncommon causes of stroke. *Brain*, *125*, 923–924.
Rubinov, M., & Sporns, O. (2010). Complex network measures of brain connectivity: Uses and interpretations. *NeuroImage*, *52*, 1059–1069.
Salvalaggio, A., de Filippo De Grazia, M., Zorzi, M., de Schotten, M. T., & Corbetta, M. (2020). Post-stroke deficit prediction from lesion and indirect structural and functional disconnection. *Brain*, *143*, 2173–2188. https://doi.org/10.1093/brain/awaa156/5861020
Saver, J. L. (2011). Optimal end points for acute stroke therapy trials: Best ways to measure treatment effects of drugs and devices. *Stroke*, *42*, 2356–2362.
Saver, J. L., Chaisinanunkul, N., Campbell, B. C. V., Grotta, J. C., Hill, M. D., Khatri, P., Landen, J., Lansberg, M. G., Venkatasubramanian, C., & Albers, G. W. (2021). Standardized nomenclature for modified ranking scale global disability outcomes: consensus recommendations from stroke therapy academic industry roundtable XI. *Stroke*, *52*, 3054–3062. https://doi.org/10.1161/STROKEAHA.121.034480
Schirmer, M. D., Ktena, S. I., Nardin, M. J., Donahue, K. L., Giese, A. K., Etherton, M. R., Wu, O., & Rost, N. S. (2019). Rich-club organization: An important determinant of functional outcome after acute ischemic stroke. *Frontiers in Neurology*, *10*, 956. https://doi.org/10.3389/fneur.2019.00956/full
Schlemm, E., Ingwersen, T., Königsberg, A., Boutitie, F., Ebinger, M., Endres, M., Fiebach, J. B., Fiehler, J., Galinovic, I., Lemmens, R., Muir, K. W., Nighoghossian, N., Pedraza, S., Puig, J., Simonsen, C. Z., Thijs, V., Wouters, A., Gerloff, C., Thomalla, G., & Cheng, B. (2021). Preserved structural connectivity mediates the clinical effect of thrombolysis in patients with anterior-circulation stroke. *Nature Communications*, *12*, 2590.
Schlemm, E., Schulz, R., Bönstrup, M., Krawinkel, L., Fiehler, J., Gerloff, C., Thomalla, G., & Cheng, B. (2020). Structural brain networks and functional motor outcome after stroke—A prospective cohort study. *Brain Communications*, *2*, 1–13.
Sinke, M. R. T., Otte, W. M., van Meer, M. P. A., van der Toorn, A., & Dijkhuizen, R. M. (2018). Modified structural network backbone in the contralesional hemisphere chronically after stroke in rat brain. *Journal of Cerebral Blood Flow and Metabolism*, *38*, 1642–1653.
Snider, S. B., Hsu, J., Darby, R. R., Cooke, D., Fischer, D., Cohen, A. L., Grafman, J. H., & Fox, M. D. (2020). Cortical lesions causing loss of consciousness are anticorrelated with the dorsal brainstem. *Human Brain Mapping*, *41*, 1520–1531. https://doi.org/10.1002/hbm.24892#.XhO8mgJBvFA.twitter
Straathof, M., Sinke, M. R. T., van der Toorn, A., Weerheim, P. L., Otte, W. M., & Dijkhuizen, R. M. (2019). Differences in structural and functional networks between young adult and aged rat brains before and after stroke lesion simulations. *Neurobiology of Disease*, *126*, 23–35.
Tate, W. J., Polding, L. C., Christensen, S., Mlynash, M., Kemp, S., Heit, J. J., Marks, M. P., Albers, G. W., & Lansberg, M. G. (2021). Predictors of early and late infarct growth in DEFUSE 3. *Frontiers in Neurology*, *12*, 699153.
Tay, J., Lisiecka-Ford, D. M., Hollocks, M. J., Tuladhar, A. M., Barrick, T. R., Forster, A., O'Sullivan, M. J., Husain, M., de Leeuw, F. E., Morris, R. G., & Markus, H. S. (2020). Network neuroscience of apathy in cerebrovascular disease. *Progress in Neurobiology*, *188*, 101785.
Team R Development Core. (2018). *A language and environment for statistical computing. R Foundation for Statistical Computing* (Vol. 2). R Foundation for Statistical Computing. http://www.r-project.org
The National Institute of Neurological Disorders and Stroke rt-PA Stroke Study Group, Zambello, R., Trentin, L., Facco, M., Cerutti, A., Sancetta, R., Milani, A., Raimondi, R., Tassinari, C., Agostini, C., & Semenzato, G. (1995). Tissue plasminogen activator for acute ischemic stroke. *The New England Journal of Medicine*, *333*, 1581–1588. https://doi.org/10.1056/NEJM199512143332401
Thomalla, G., Simonsen, C. Z., Boutitie, F., Andersen, G., Berthezene, Y., Cheng, B., Cheripelli, B., Cho, T.-H., Fazekas, F., Fiehler, J., Ford, I., Galinovic, I., Gellissen, S., Golsari, A., Gregori, J., Günther, M., Guibernau, J., Häusler, K. G., Hennerici, M., … Gerloff, C. (2018). MRI-guided thrombolysis for stroke with unknown time of onset. *The New England Journal of Medicine*, *379*, 611–622. https://doi.org/10.1056/NEJMoa1804355
Tozlu, C., Jamison, K., Gu, Z., Gauthier, S. A., & Kuceyeski, A. (2021). Estimated connectivity networks outperform observed connectivity networks when classifying people with multiple sclerosis into disability groups. *NeuroImage: Clinical*, *32*, 102827.
Umarova, R., & Thomalla, G. (2020). Indirect connectome-based prediction of post-stroke deficits: Prospects and limitations. *Brain*, *143*, 1966–1970.
van den Heuvel, M. P., Kahn, R. S., Goñi, J., & Sporns, O. (2012). High-cost, high-capacity backbone for global brain communication. *Proceedings of the National Academy of Sciences of the United States of America*, *109*, 11372–11377.
Wilson, E. B. (1927). Probable inference, the law of succession, and statistical inference. *Journal of the American Statistical Association*, *22*, 209–212.
Xu, X., Tang, R., Zhang, L., & Cao, Z. (2019). Altered topology of the structural brain network in patients with poststroke depression. *Frontiers in Neuroscience*, *13*, 776.
Yourganov, G., Fridriksson, J., Rorden, C., Gleichgerrcht, E., & Bonilha, L. (2016). Multivariate connectome-based symptom mapping in post-stroke patients: Networks supporting language and speech. *The Journal of Neuroscience*, *36*, 6668–6679.
Zalesky, A., Fornito, A., & Bullmore, E. T. (2010). Network-based statistic: Identifying differences in brain networks. *NeuroImage*, *53*, 1197–1207.
Zangerle, A., Kiechl, S., Spiegel, M., Furtner, M., Knoflach, M., Werner, P., Mair, A., Wille, G., Schmidauer, C., Gautsch, K., Gotwald, T., Felber, S., Poewe, W., & Willeit, J. (2007). Recanalization after thrombolysis in stroke patients: Predictors and prognostic implications. *Neurology*, *68*, 39–44.
Zhang, J., Zhang, Y., Xing, S., Liang, Z., & Zeng, J. (2012). Secondary neurodegeneration in remote regions after focal cerebral infarction: A new target for stroke management? *Stroke*, *43*, 1700–1705. https://doi.org/10.1161/STROKEAHA.111.632448
Zhou, X., Hu, X., Zhang, C., Wang, H., Zhu, X., Xu, L., Sun, Z., & Yu, Y. (2016). Aberrant functional connectivity and structural atrophy in subcortical vascular cognitive impairment: Relationship with cognitive impairments. *Frontiers in Aging Neuroscience*, *8*, 14.

SUPPORTING INFORMATION

Additional supporting information can be found online in the Supporting Information section at the end of this article.

How to cite this article: Schlemm, E., Jensen, M., Kuceyeski, A., Jamison, K., Ingwersen, T., Mayer, C., Königsberg, A., Boutitie, F., Ebinger, M., Endres, M., Fiebach, J. B., Fiehler, J., Galinovic, I., Lemmens, R., Muir, K. W., Nighoghossian, N., Pedraza, S., Puig, J., Simonsen, C. Z., … Cheng, B. (2022). Early effect of thrombolysis on structural brain network organisation after anterior-circulation stroke in the randomized WAKE-UP trial. *Human Brain Mapping*, *43*(16), 5053–5065. https://doi.org/10.1002/hbm.26073